Classical Theory of the Ground Spin-State in Normal Tetragonal Spinels. I. Néel, Yafet-Kittel, and Collinear Antiferromagnetic Modes

N. MENYUK, K. DWIGHT, D. LYONS,* AND T. A. KAPLAN
Lincoln Laboratory,† Massachusetts Institute of Technology, Lexington, Massachusetts
(Received April 23, 1962)

An appreciable number of magnetic materials with the spinel structure exhibit tetragonal symmetry, rather than cubic, in their x-ray diffraction patterns. Because of the distortion, five different nearest-neighbor exchange interactions are possible, so that four ratios (t, u, v, and w) amongst these interactions are required for the characterization of such a material. In this paper, we use the generalized Luttinger-Tisza method (GLT) to determine rigorously the ranges of values of the above ratios (regions in t, u, v, w parameter space) for which the familiar Néel, Yafet-Kittel, and collinear antiferromagnetic spin configurations ($\mathbf{k}=0$ modes) are the ground states of the classical Heisenberg exhange energy. We also determine the characteristic k vectors of the spin deviations which destabilize the $\mathbf{k}=0$ modes along the boundary surfaces of their ground-state regions. Such information is important as a first step towards a more complete investigation of ground-state spin configurations in tetragonal spinels.

We find the above ground-state regions to be significantly smaller than would be predicted on the basis of a sublattice model. Consequently, knowledge of the actual spin configuration can place important restrictions upon the relative strengths of exchange interactions, as in the case of copper chromite. In addition, we find that the destabilizing k vector is not always parallel to a symmetry direction, even for nearly-cubic spinels.

In this paper, we also use the molecular-field approximation to investigate the relative stabilities of the $\mathbf{k}=0$ mode in the neighborhood of the highest magnetic transition temperature (T_c). We find that the only possible ferrimagnetic configuration at T_c is of the Néel type, and for moderate degrees of distortion, its stability region is much larger at T_c than in the ground state. This result implies that at least two magnetic transitions must occur in any spinel with a magnetic noncollinear ground state.

I. INTRODUCTION

As a means of achieving an understanding of exchange interactions, the magnetic properties of materials with the spinel structure have been of considerable interest in recent years. A knowledge of the magnetic ground state in these materials is necessary for any valid interpretation of the experimental data. Néel[1] achieved considerable success in interpreting a large body of such data on ferrites[2] by assuming a model in which all the spins on the tetrahedral (A) sites are parallel, with the spins on the octahedral (B) sites antiparallel to those on the A sites. However, the results of other magnetic measurements, notably on chromites with the spinel structure,[2] could not be understood on the basis of his model.

To overcome this difficulty, Yafet and Kittel[3] generalized the two sublattices of the Néel model to six sublattices corresponding to the two A sites and four B sites in the translational primitive unit cell of the spinel structure. They showed that, for a sufficiently large antiferromagnetic B-B interaction, a new "triangular" spin mode yielded a lower energy than the Néel configuration. Although this "triangular" mode could account for the observed values of low-temperature magnetizations, Kaplan[4,5] later showed by perturbation methods that it is never stable in cubic spinels having only nearest-neighbor A-B and B-B interactions. He found that, upon increasing the antiferromagnetic B-B interaction, the Néel mode is destabilized by spin deviations characterized by a wave vector along a [110] direction with a definite characteristic wavelength.

Using this information, together with the Lyons-Kaplan[6] generalization of the Luttinger-Tisza method (GLT), Lyons, Kaplan, Dwight, and Menyuk[7] have recently shown that a spin configuration having the form of a ferrimagnetic spiral propagating in the [110] direction is probably the ground state in cubic spinels (spinels with exchange constants J_{ij} that are invariant under all the cubic operations) for a certain range of B-B interactions. This spiral has appreciably lower energy than the Yafet-Kittel configurations, and appears to be substantiated by the neutron diffraction results recently reported by Corliss and Hastings[8] for manganese chromite. The spiral model also yields insight into the temperature dependence of the magnetization of cobalt chromite.[9]

Although the Yafet-Kittel model is not applicable to cubic spinels, Prince[10] has found evidence for their "triangular" mode from the diffraction of neutrons by copper chromite, which is a tetragonal spinel. His findings were later corroborated and amplified by Nathans, Pickart, and Miller.[11] Furthermore, Kaplan, Dwight, and Menyuk[12] had considered the theoretical effect of tetragonal distortion in spinels and found the Yafet-

---

* Present address: Sperry-Rand Research Center, Sudbury, Massachusetts.

† Operated with support from the U. S. Army, Navy, and Air Force.

[1] L. Néel, Ann. Phys. **3**, 137 (1948).
[2] E. W. Gorter, Philips Research Repts. **9**, 295, 321, 403 (1954).
[3] Y. Yafet and C. Kittel, Phys. Rev. **87**, 290 (1952).
[4] T. A. Kaplan, Phys. Rev. **116**, 888 (1959).
[5] T. A. Kaplan, Phys. Rev. **119**, 1460 (1960).
[6] D. Lyons and T. A. Kaplan, Phys. Rev. **120**, 1580 (1960).
[7] D. Lyons, T. A. Kaplan, K. Dwight, and N. Menyuk, Phys. Rev. **126**, 540 (1962).
[8] L. Corliss and J. Hastings, Suppl. J. Appl. Phys. **33**, 1138 (1962). J. Hastings and L. Corliss, Phys. Rev. **126**, 556 (1962).
[9] N. Menyuk, A. Wold, D. Rogers, and K. Dwight, Suppl. J. Appl. Phys. **33**, 1144 (1962).
[10] E. Prince, Acta Cryst. **10**, 554 (1957).
[11] R. Nathans, S. J. Pickart, and A. Miller, Bull. Am. Phys. Soc. **6**, 54 (1961).
[12] T. A. Kaplan, K. Dwight, and N. Menyuk, Bull. Am. Phys. Soc. **5**, 460 (1960).

Kittel modes to be stable for limited ranges of A-B and B-B interactions. They also found that the Néel mode could be stable only for a sharply restricted range of interactions. Subsequent application of the GLT method to this problem (tetragonal spinels without A-A interactions) by Kaplan, Dwight, Lyons, and Menyuk[13] led to more definitive outer bounds for the stability regions of the Néel and Yafet-Kittel configurations, as well as to some information concerning the directions of the destabilizing wave vectors. However, neither the explicit boundary equations nor the calculational details were presented at that time.

In this paper we shall consider the ground spin-state problem ($T=0°$K) for normal tetragonal spinels (normal spinels with exchange constants J_{ij} which are invariant under all the symmetry operations of the tetragonal space group $I4_1/amd$) possessing nearest-neighbor A-A, A-B, and B-B exchange interactions. Thus, the results described in reference 13 will be obtainable as special cases of the more general calculations presented here. Our present investigation is directed towards a determination of the regions (in a space which describes the ratios of the various exchange interactions) where the Néel and Yafet-Kittel configurations are the ground state, and towards a determination of the directions of the destabilizing characteristic wave vectors along the boundary surfaces. As illustrated by the treatment of cubic spinels,[7] this latter information is important in the construction of configurations which may be the ground state outside of the Néel and Yafet-Kittel stability regions. In addition to the ground-state problem, we shall also consider the stability regions of the Néel and Yafet-Kittel modes at the Curie point ($T=T_c$) by means of the molecular-field approximation. The fact that the low and high temperature boundaries do not coincide suggests the possibility of magnetic transitions.

II. THEORETICAL FOUNDATIONS

It is convenient to express the classical Heisenberg exchange energy in the form

$$E=\sum_{n\nu,m\mu}\bar{J}_{n\nu,m\mu}\mathbf{S}_{n\nu}\cdot\mathbf{S}_{m\mu}, \tag{1}$$

where $\mathbf{S}_{n\nu}$ and $\mathbf{S}_{m\mu}$ are unit vectors which define the directions of the classical spins at the lattice positions $\mathbf{R}_{n\nu}$ and $\mathbf{R}_{m\mu}$, respectively, and $\bar{J}_{n\nu,m\mu}$ is the product of the usual exchange parameter connecting these sites with the magnitudes of the appropriate spins. The subscripts ν and μ define the site locations within the particular primitive unit cells defined by n and m, where $n, m=1, 2, \cdots N$.

In the normal spinel lattice, there are two tetrahedral (A) sites (occupied by one ionic species) and four octahedral (B) sites (occupied by some other ionic species) per primitive unit cell, these six sites being identified by ν, $\mu=1, 2, \cdots 6$ as shown in Fig. 1. In tetragonally distorted normal spinels, there can be as many as five different nearest-neighbor exchange constants: $\bar{J}_{AA}=J_{AA}S_A^2$ for all A-A interactions; $\bar{J}_{AB}=J_{AB}S_AS_B$ for A-B interactions between pairs connected by vectors parallel to such (face-centered tetragonal) directions as the [311], [131], etc., and $\bar{J}_{AB}'$ for similar pairs along the [113], etc.; $\bar{J}_{BB}=J_{BB}S_B^2$ for B-B interactions between pairs along the [110] and [1$\bar{1}$0], and $\bar{J}_{BB}'$ for similar pairs along the [101], [011], etc. Thus, the tetragonal distortion results in a differentiation between two distinct types of A-B interactions and between two distinct types of B-B interactions, as indicated in Fig. 2.

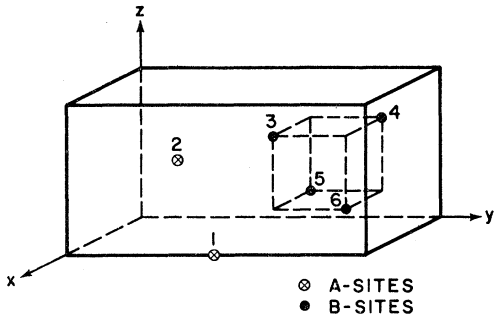

FIG. 1. The sites in a primitive unit cell of the spinel structure. The numbers $\nu=1, 2, \cdots, 6$ identify the particular sites.

The ground-state spin configuration is that set of values for the many ($\approx 10^{23}$) variables $S_{n\nu}$ which minimizes Eq. (1) subject to the "strong constraints" that all the $\mathbf{S}_{n\nu}$ be unit vectors, i.e.,

$$\mathbf{S}_{n\nu}\cdot\mathbf{S}_{n\nu}=1. \tag{2}$$

Clearly, the Heisenberg energy E will be a minimum whenever the dimensionless energy E', defined by

$$E'=E/(2J_{AB}+J_{AB}')S_AS_B=E/(2\bar{J}_{AB}+\bar{J}_{AB}'), \tag{3}$$

is a minimum, provided only that the net A-B inter-

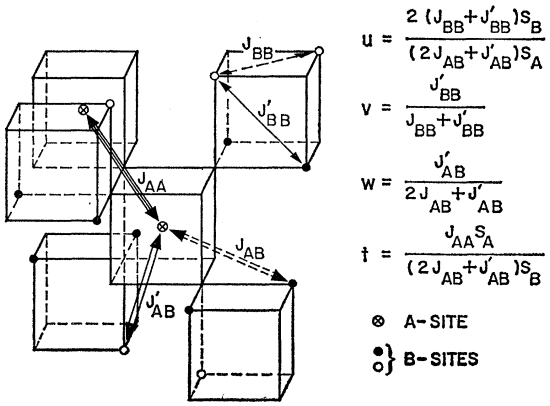

FIG. 2. Possible nearest-neighbor exchange interactions conforming to tetragonal symmetry.

[13] T. A. Kaplan, K. Dwight, D. Lyons, and N. Menyuk, Suppl. J. Appl. Phys. 32, 13s (1961).

action is antiferromagnetic ($2\bar{J}_{AB}+\bar{J}_{AB}'>0$), which we will assume. It is then apparent that the ground-state problem depends only on the four dimensionless parameters which define E', these parameters being given by the following ratios of the exchange constants and spin magnitudes:

$$\begin{aligned} t&=J_{AA}S_A/[(2J_{AB}+J_{AB}')S_B], \\ u&=2(J_{BB}+J_{BB}')S_B/[(2J_{AB}+J_{AB}')S_A], \\ v&=J_{BB}'/(J_{BB}+J_{BB}'), \\ w&=J_{AB}'/(2J_{AB}+J_{AB}'). \end{aligned} \tag{4}$$

Any tetragonal spinel with only "nearest-neighbor" interactions is characterized by a point in the above four-dimensional parameter space. We note in passing that t and u describe the strength of the A-A and B-B interactions relative to the net A-B interaction, whereas v and w describe the tetragonal differentiation between the two types of B-B and the two types of A-B interactions, respectively.

The GLT method developed by Lyons and Kaplan[6] is the simplest known technique for rigorously determining the ground state of Eqs. (1) or (3) for the spinel structure. This method utilizes the tractable problem of minimizing the exchange energy over all sets of $\mathbf{S}_{n\nu}$ which satisfy the "weak constraint"

$$\sum_{n\nu}\beta_\nu^{-2}\mathbf{S}_{n\nu}\cdot\mathbf{S}_{n\nu}=N\sum_\nu\beta_\nu^{-2}, \tag{5}$$

where the β_ν are adjustable parameters.[6] For any set of β_ν, the weak constraint of Eq. (5) is automatically satisfied by *all* configurations which satisfy the strong constraints of Eq. (2) (i.e., by *all* physical configurations), although the converse is not true. Hence, the configurations which minimize the energy subject to any particular weak constraint must necessarily possess lower energy than *any* (other) physical configuration. In general, such a minimum-energy configuration will not always satisfy the strong constraints. However, it is sometimes possible, as demonstrated in the succeeding sections of this paper, to find a set of numbers β_ν such that the minimum-energy configuration over the resulting weak constraint does satisfy the strong constraints, and hence is itself a physical configuration. Then it follows *rigorously* from the above argument that this particular configuration must be the ground state of the Heisenberg exchange energy.

By expressing the spin vectors $\mathbf{S}_{n\nu}$ in terms of their Fourier transforms,

$$\mathbf{S}_{n\nu}=\sum_{\mathbf{k}}\mathbf{Q}_\nu(\mathbf{k})\exp(i\mathbf{k}\cdot\mathbf{R}_{n\nu}), \tag{6}$$

it can be shown[6] that all the extrema of the energy E', and hence those of E, over the weak constraint of Eq. (5) must satisfy the eigenvalue equation

$$\sum_\nu\mathfrak{L}_{\nu\mu}'(\mathbf{k})\beta_\mu^{-1}\mathbf{Q}_\mu(\mathbf{k})=\lambda\beta_\nu^{-1}\mathbf{Q}_\nu(\mathbf{k}), \tag{7}$$

the resulting energy being

$$E'=N\lambda\sum_\nu\beta_\nu^{-2}. \tag{8}$$

Here the matrix $\mathfrak{L}'(\mathbf{k})$ is defined by $\mathfrak{L}_{\nu\mu}'(\mathbf{k})=\beta_\nu\beta_\mu L_{\nu\mu}'(\mathbf{k})$, where

$$(2\bar{J}_{AB}+\bar{J}_{AB}')L_{\nu\mu}'(\mathbf{k})=\sum_m\bar{J}_{n\nu,m\mu}\times\exp[i\mathbf{k}\cdot(\mathbf{R}_{m\mu}-\mathbf{R}_{n\nu})]. \tag{9}$$

For a tetragonal spinel, this expression gives

$$L'=(\mathbf{k})\begin{bmatrix} 0 & t\chi & \eta_1 & \eta_2 & \eta_3 & \eta_4 \\ t\chi^* & 0 & \eta_1^* & \eta_2^* & \eta_3^* & \eta_4^* \\ \eta_1^* & \eta_1 & 0 & u(1-v)\zeta_{12} & uv\zeta_{13} & uv\zeta_{14} \\ \eta_2^* & \eta_2 & u(1-v)\zeta_{12} & 0 & uv\zeta_{23} & uv\zeta_{24} \\ \eta_3^* & \eta_3 & uv\zeta_{13} & uv\zeta_{23} & 0 & u(1-v)\zeta_{34} \\ \eta_4^* & \eta_4 & uv\zeta_{14} & uv\zeta_{24} & u(1-v)\zeta_{34} & 0 \end{bmatrix}, \tag{10}$$

where χ, η_i, and ζ_{ij} are given as explicit functions of w and $\mathbf{k}$ in Appendix I. The minimum eigenvalue of $\mathfrak{L}'(\mathbf{k})$ (minimum over the six branches $\alpha=1, 2, \cdots 6$ and over all $\mathbf{k}$ in the first Brillouin zone) yields the minimum value of the energy E' over all configurations which satisfy the weak constraint.

This minimum eigenvalue $\lambda_{\min}$ may occur for different branches and different k vectors, i.e., for a degenerate set of $\lambda_{\alpha'}(\mathbf{k}')=\lambda_{\min}$, each of which is associated with a normalized eigenvector $\mathbf{\Psi}_{\alpha'}(\mathbf{k}')$ whose components are $\Psi_{\alpha'\nu}(\mathbf{k}')$. Here $\lambda_\alpha(\mathbf{k})$, $\alpha=1, \cdots, 6$ is the set of eigenvalues of $\mathfrak{L}'(\mathbf{k})$, for given $\mathbf{k}$. Then the corresponding spin configurations are those constructed from Fourier transforms given by

$$\mathbf{Q}_\nu(\mathbf{k}')=\sum_{\alpha'}\beta_\nu\Psi_{\alpha'\nu}(\mathbf{k}')C_{\alpha'}(\mathbf{k}'), \tag{11}$$

where $C_\alpha(\mathbf{k})=0$ when $\lambda_\alpha(\mathbf{k})\neq\lambda_{\min}$, and where the weak constraint requires only that

$$\sum_{\alpha'\mathbf{k}'}\mathbf{C}_{\alpha'}{}^*(\mathbf{k}')\cdot\mathbf{C}_{\alpha'}(\mathbf{k}')=\sum_\nu\beta_\nu^{-2}. \tag{12}$$

If these vectors $\mathbf{C}_{\alpha'}(\mathbf{k}')$ can be chosen so that the constructed configuration also satisfies the strong constraints, then the resulting physical configuration is the ground state of the Heisenberg energy.

In the practical application of the GLT method, it is frequently convenient to depart slightly from the formal approach stated above by initially considering some restricted set of k vectors, say $\mathbf{k}_i$, and their associated matrices $\mathfrak{L}'(\mathbf{k}_i)$. Configurations are constructed from the minimum eigenvector(s) of these matrices, and then the β_ν are determined so that one of these configurations

satisfies the strong constraints. Finally, the general matrices $\mathfrak{L}'(\mathbf{k})$ obtained with this particular set of β_ν are investigated over all $\mathbf{k}$ in the first Brillouin zone, the constructed configuration being the ground state whenever the minimum eigenvalue of the special matrices $\mathfrak{L}'(\mathbf{k}_i)$ remains the absolute minimum over all $\mathfrak{L}'(\mathbf{k})$.

Our present investigation concerns the Néel and Yafet-Kittel configurations, which contain only $\mathbf{k}=0$ Fourier components. Accordingly, we shall initially consider the special matrix $\mathfrak{L}'(0)$, for which the expressions given in Appendix I yield $\chi(0)=4$, $\eta_i(0)=\zeta_{ij}(0)=1$. Since the resulting structure of the matrix $\mathbf{L}'(0)$ obtained from Eq. (10) is symmetric between the two A sites and among the four B sites, we shall tentatively choose

$$\beta_1=\beta_2=1,$$
$$\beta_3=\beta_4=\beta_5=\beta_6=\beta. \tag{13}$$

In other words, the symmetry of $\mathbf{L}'(0)$ suggests that a single adjustable parameter β might suffice in the construction of a configuration which yields the minimum eigenvalue of $\mathfrak{L}'(0)$ and simultaneously satisfies the strong constraints. Although we shall see that this choice does suffice for the present problem, it should be pointed out that there is no guarantee that symmetry considerations will always lead to a satisfactory set of β_ν.[7]

With the β_ν given by Eq. (13), it follows that

$$\mathfrak{L}'(0)=\begin{bmatrix} 0 & 4t & \beta & \beta & \beta & \beta \\ 4t & 0 & \beta & \beta & \beta & \beta \\ \beta & \beta & 0 & \beta^2u(1-v) & \beta^2uv & \beta^2uv \\ \beta & \beta & \beta^2u(1-v) & 0 & \beta^2uv & \beta^2uv \\ \beta & \beta & \beta^2uv & \beta^2uv & 0 & \beta^2u(1-v) \\ \beta & \beta & \beta^2uv & \beta^2uv & \beta^2u(1-v) & 0 \end{bmatrix}. \tag{14}$$

The eigenvalues λ_α and associated eigenvectors $\mathbf{\Psi}_\alpha$ ($\alpha=1, 2, \cdots 6$) of this matrix are given explicitly in Table I, where only the positive branch of the square root is to be taken, and where

$$\rho=4t+\beta^2u(1+v),$$
$$\sigma=4t-\beta^2u(1+v). \tag{15}$$

Furthermore, since $\mathfrak{L}'(0)\mathbf{\Psi}_\alpha=\lambda_\alpha\mathbf{\Psi}_\alpha$, it can easily be shown that

$$a_\alpha=(\lambda_\alpha-4t)/(4\beta). \tag{16}$$

The explicit determination of $\beta(t,u,v,w)$ such that a physical configuration can be constructed from the minimum eigenvector(s) of the matrix $\mathfrak{L}'(0)$ is left to the next section, and the investigation of the corresponding matrices $\mathfrak{L}'(\mathbf{k})$ to the succeeding one.

III. FORMULATION OF $k=0$ MODES

In the preceding section, it has been shown that the use of the GLT method to investigate the classical ground state involves a set of matrices $\mathfrak{L}'(\mathbf{k})$ which are matrix functions of the exchange parameters t, u, v, and w. In order to define such a set of matrices, a number β must first be chosen as some explicit function of t, u, v, and w. The choice of $\beta(t,u,v,w)$ is dictated by the requirement that some particular physical spin configuration (configuration satisfying the strong constraints) yield an energy extrema over the weak constraint, or equivalently, that the configuration in question correspond to some eigenvector(s) of the appropriate $\mathfrak{L}'(\mathbf{k})$. Accordingly, we shall now proceed to formulate the $\mathbf{k}=0$ modes in terms of eigenvectors of $\mathfrak{L}'(0)$ in order to determine their associated $\beta(t,u,v,w)$, noting that these eigenvectors must arise from the minimum $\lambda_\alpha(0)$ to be of interest.

TABLE I. Eigenvalues and associated eigenvectors of $\mathfrak{L}'(0)$.

α	λ_α	$\mathbf{\Psi}_\alpha$
1	$\frac{1}{2}[\rho-(\sigma^2+32\beta^2)^{1/2}]$	$(2+4a_1^2)^{-1/2}(1,1,a_1,a_1,a_1,a_1)$
2	$-\beta^2u(1-v)$	$(1/\sqrt{2})(0, 0, 1, -1, 0, 0)$
3	$-\beta^2u(1-v)$	$(1/\sqrt{2})(0, 0, 0, 0, 1, -1)$
4	$\beta^2u(1-3v)$	$(1/2)(0, 0, 1, 1, -1, -1)$
5	$-4t$	$(1/\sqrt{2})(1, -1, 0, 0, 0, 0)$
6	$\frac{1}{2}[\rho+(\sigma^2+32\beta^2)^{1/2}]$	$(2+4a_6^2)^{-1/2}(1,1,a_6,a_6,a_6,a_6)$

A. Néel Configuration ($\mathcal{S}_N$)

In the Néel configuration ($\mathcal{S}_N$), all the spins are parallel to some direction, say, $\hat{z}'$, with $\mathbf{S}_{n\nu}=\hat{z}'$ for $\nu=1, 2$ and $\mathbf{S}_{n\nu}=-\hat{z}'$ for $\nu=3, 4, 5, 6$. It follows from Eqs. (6) and (11) that the corresponding eigenvector, apart from normalization, must be given by $\mathbf{\Psi}_N=(1, 1, -1/\beta, -1/\beta, -1/\beta, -1/\beta)$. Furthermore, $\mathbf{\Psi}_N$ must be identical with some $\mathbf{\Psi}_\alpha$ from Table I in order for $\mathcal{S}_N$ to yield an extrema over the weak constraint. In particular, the condition $\mathbf{\Psi}_N=\mathbf{\Psi}_1$ requires merely that $\beta a_1=-1$. Then it follows from Eq. (16) that λ_1 for $\mathcal{S}_N$ will be given explicitly by

$$\lambda_N=-4(1-t), \tag{17}$$

and comparison with Table I shows that this result can be obtained only if β is chosen so that

$$\beta_N{}^2=4(1-t)/[2-u(1+v)]. \tag{18}$$

Here the subscript N is used to emphasize the point that these expressions for $\lambda(t,u,v,w)$ are specifically associated with the Néel configuration.

For the particular choice $\beta=\beta_N$, it can be seen from Table I that λ_N is the minimum eigenvalue of $\mathfrak{L}'(0)$

whenever simultaneously $2t\leq 1$, $u\leq 1$, and $2uv\leq 1$. These inequalities define that region in parameter space within which $\mathcal{S}_N$ would be stable if only $\mathbf{k}=0$ were considered (giving an extension of the Yafet-Kittel theory to tetragonal spinels). Along the boundaries of this region, various eigenvalue branches become degenerate with $\lambda_1=\lambda_N$: λ_2 and λ_3 for $u=1$, λ_4 for $2uv=1$, and λ_5 for $2t=1$; outside of this region, the indicated branches lie lower than λ_1.

B. Yafet-Kittel Configurations ($\mathcal{S}_{Yi}$)

There are three basic types of Yafet-Kittel triangular spin configurations[3,14] which will be denoted by $\mathcal{S}_{Y1}$, $\mathcal{S}_{Y2}$, $\mathcal{S}_{Y3}$. Being coplanar, these configurations can be expressed in terms of spin components along two arbitrary orthogonal directions, say $\hat{z}'$ and $\hat{x}'$, where nonzero x' components can occur either for the A sites or for the B sites, but not both simultaneously.[3,14] From Eqs. (6) and (11), it can be seen that the z' and x' components cannot be obtained from a single eigenvector, but must arise from different eigenvectors $\mathbf{\Psi}(z')$ and $\mathbf{\Psi}(x')$. Furthermore, the condition that the corresponding Yafet-Kittel configuration be an extrema over the weak constraint requires not only that $\mathbf{\Psi}(z')$ and $\mathbf{\Psi}(x')$ be identical with eigenvectors $\mathbf{\Psi}_\alpha$ and $\mathbf{\Psi}_{\alpha'}$ of $\mathfrak{L}'(0)$, but also that $\lambda_\alpha=\lambda_{\alpha'}$, since it was shown in Sec. II that only degenerate eigenvectors can be combined. Such necessary degeneracies occur "by accident" along the boundary surfaces discussed in Sec. III A, but can more generally be "forced"[6] by an appropriate choice of $\beta(t,u,v,w)$.

1. The configurations $\mathcal{S}_{Y1}$ can be defined as having $\mathbf{S}_{n\nu}=\hat{z}'$ for $\nu=1, 2$; $\mathbf{S}_{n\nu}=-\hat{z}'\cos\theta+\hat{x}'\sin\theta$ for $\nu=3,4$; $\mathbf{S}_{n\nu}=-\hat{z}'\cos\theta-\hat{x}'\sin\theta$ for $\nu=5, 6$. Then consideration of Eqs. (6) and (11) yields the (unnormalized) eigenvectors $\mathbf{\Psi}_{Y1}(z')=(1, 1, -\beta^{-1}\cos\theta, -\beta^{-1}\cos\theta, -\beta^{-1}\cos\theta, -\beta^{-1}\cos\theta)$ and $\mathbf{\Psi}_{Y1}(x')=(0, 0, 1, 1, -1, -1)$. From Table I, it is clear that $\mathbf{\Psi}_{Y1}(x')=\mathbf{\Psi}_4$ and $\mathbf{\Psi}_{Y1}(z')=\mathbf{\Psi}_1$ with θ determined by $\cos\theta=-\beta a_1$. Thus, $\mathcal{S}_{Y1}$ results from the use of $\mathbf{C}_1=\hat{z}'(2+4\beta^{-2}\cos^2\theta)^{1/2}$ and $\mathbf{C}_4=\hat{x}'2\beta^{-1}\sin\theta$ in Eq. (11). Then it only remains to fulfill the required degeneracy condition that $\lambda_1=\lambda_4$ by chosing β so that

$$\beta_{Y1}^2=(4tuv-2)/[u^2v(1-3v)], \tag{19}$$

which choice yields

$$\lambda_{Y1}=(4tuv-2)/uv, \tag{20}$$

$$\cos\theta=(2uv)^{-1}. \tag{21}$$

Since θ must be a physical angle in order to satisfy the strong constraints, this solution can exist only if $2uv\geq 1$. In addition, a consideration of Table I for the choice $\beta=\beta_{Y1}$ shows that λ_{Y1} is the minimum eigenvalue of $\mathfrak{L}'(0)$ only when $2v\geq 1$ and also $4tuv\leq 1$ (λ_2 and λ_3 become degenerate with λ_{Y1} when $2v=1$, λ_5 when $4tuv=1$). Only inside the region defined by $2uv\geq 1$, $2v\geq 1$, and $4tuv\leq 1$ is it possible to choose a $\beta(t,u,v,w)$ so that the minimum eigenvectors of $\mathfrak{L}'(0)$ correspond to $\mathcal{S}_{Y1}$.

2. The configuration $\mathcal{S}_{Y2}$ can be defined as having $\mathbf{S}_{n\nu}=\hat{z}'$ for $\nu=1, 2$; $\mathbf{S}_{n\nu}=-\hat{z}'\cos\phi+\hat{x}'\sin\phi$ for $\nu=3, 5$ or $3, 6$; $\mathbf{S}_{n\nu}=-\hat{z}'\cos\phi-\hat{x}'\sin\phi$ for $\nu=4, 6$ or $4, 5$. From Eqs. (6) and (11) together with Table I, it follows that (apart from normalization) the appropriate eigenvectors are $\mathbf{\Psi}_{Y2}(x')=\mathbf{\Psi}_2\pm\mathbf{\Psi}_3$ and $\mathbf{\Psi}_{Y2}(z')=\mathbf{\Psi}_1$ with $\cos\phi=-\beta a_1$. Upon satisfying the degeneracy requirement that $\lambda_1=\lambda_2=\lambda_3$, one obtains explicitly

$$\beta_{Y2}^2=4(1-tu)/[u^2(1-v)], \tag{22}$$

$$\lambda_{Y2}=-4(1-tu)/u, \tag{23}$$

$$\cos\phi=u^{-1}. \tag{24}$$

Considerations similar to those above show that $\beta(t,u,v,w)$ can be chosen to yield $\mathcal{S}_{Y2}$ from the minimum eigenvectors of $\mathfrak{L}'(0)$ only in a region where $u\geq 1$, $2v\leq 1$, and $2tu\leq 1$. Here the boundary $u=1$ arises from the strong constraints, $2v=1$ from degeneracy of λ_4 with λ_{Y2}, and $2tu=1$ from $\lambda_5=\lambda_{Y2}$.

3. The configuration $\mathcal{S}_{Y3}$ can be defined as having $\mathbf{S}_{n1}=\hat{x}'\cos\psi+\hat{x}'\sin\psi$, $\mathbf{S}_{n2}=\hat{z}'\cos\psi-\hat{x}'\sin\psi$ and, $\mathbf{S}_{n\nu}=-\hat{z}'$ for $\nu=3, 4, 5, 6$. Normalization being ignored as before, our procedure gives $\mathbf{\Psi}_{Y3}(x')=\mathbf{\Psi}_5$ and $\mathbf{\Psi}_{Y3}(z')=\mathbf{\Psi}_1$ with $\cos\psi=-(\beta a_1)^{-1}$. The determination of β from the condition that $\lambda_1=\lambda_5$ yields

$$\beta_{Y3}^2=4t^2/(1-tu-tuv), \tag{25}$$

$$\lambda_{Y3}=-4t, \tag{26}$$

$$\cos\psi=(2t)^{-1}. \tag{27}$$

Then the appropriate region for $\mathcal{S}_{Y3}$ is defined by the following inequalities: $2t\geq 1$ in order to satisfy the strong constraints, $2tu\leq 1$ in order that $\lambda_{Y3}\leq\lambda_2=\lambda_3$, and $4tuv\leq 1$ in order that $\lambda_{Y3}\leq\lambda_4$.

From the foregoing discussions, it can be seen that the Néel and Yafet-Kittel configurations arise from the minimum eigenvector(s) of $\mathfrak{L}'(0)$ if and only if $2tu\leq 1$ and $4tuv\leq 1$, which constitute the tetragonal generalization of Lotgering's condition $\alpha\beta\leq 1$.[14] The former inequality is the more stringent when $2v<1$, the latter when $2v>1$.

C. Antiferromagnetic Configurations ($\mathcal{S}_{Ai}$)

There are two types of configurations in which the A sites are antiparallel to each other and simultaneously the B sites are antiparallel amongst themselves. The B-site eigenvector is just $\mathbf{\Psi}_4$ in $\mathcal{S}_{A1}$ and $\mathbf{\Psi}_2\pm\mathbf{\Psi}_3$ in $\mathcal{S}_{A2}$, the A-site eigenvector is $\mathbf{\Psi}_5$ in both cases, and the determination of appropriate vectors $\mathbf{C}_\alpha$ is trivial. Upon forcing the degeneracy $\lambda_4=\lambda_5$, it follows that

$$\beta_{A1}^2=4t/[u(3v-1)], \tag{28}$$

$$\lambda_{A1}=-4t. \tag{29}$$

[14] F. K. Lotgering, Philips Research Repts. 11, 190 (1956).

For the particular choice $\beta=\beta_{A1}$, the conditions that $\lambda_{A1}\leq\lambda_1$ and $\lambda_{A1}\leq\lambda_2=\lambda_3$ yield, respectively, the inequalities $4tuv\leq 1$ and $2v\geq 1$, which define the parameter region associated with S_{A1}. Similarly, forcing the degeneracy $\lambda_2=\lambda_3=\lambda_5$ results in

$$\beta_{A2}^2=4t/[u(1-v)], \tag{30}$$

$$\lambda_{A2}=-4t. \tag{31}$$

For this choice of β, the conditions are $\lambda_{A2}\leq\lambda_1$ and $\lambda_{A2}\leq\lambda_4$ and yield $2tu\geq 1$ and $2v\leq 1$ for S_{A2}.

The six $\mathbf{k}=0$ modes discussed in this section serve to completely fill[15] our t-u-v-w parameter space with physical configurations associated with the minimum eigenvector(s) of their corresponding matrices $\mathfrak{D}'(0)$. The specific choices of β given above also determine all the corresponding matrices $\mathfrak{D}'(\mathbf{k})$, which must now be investigated throughout the first Brillouin zone.

IV. GROUND-STATE REGIONS OF $k=0$ MODES

In the preceding section, we have solved the minimum energy problem posed by the simple Yafet-Kittel theory, with appropriately generalized interaction parameters (i.e., we have found the lowest $\mathbf{k}=0$ configurations). However, much more important than just obtaining such a solution is the expression of this solution in terms of the formalism of the GLT theory, since this expression enables us to determine if and where in parameter space the various configurations are actually the ground state. Specifically, we have itemized the six possible $\mathbf{k}=0$ spin configurations which yield energy extrema over appropriate weak constraints and simultaneously satisfy the strong constraints, the particular choices for $\beta(t,u,v,w)$ which yield these particular weak constraints, and the resulting eigenvalues $\lambda_{\min}(0)$. As shown in Sec. II, the GLT method now asserts that such a configuration will be the classical ground state within any region $\mathfrak{R}$ of our parameter space where its associated eigenvalue $\lambda_{\min}(0)$ remains the minimum eigenvalue of all the matrices $\mathfrak{D}'(\mathbf{k})$ defined by its particular $\beta(t,u,v,w)$, i.e., wherever

$$\lambda_{\min}(0)\leq\lambda_\alpha(\mathbf{k}) \tag{32}$$

for all six branches α and for all wave vectors $\mathbf{k}$ in the first Brillouin zone. Furthermore, since the $\mathbf{k}=0$ configurations can all be coplanar, they are locally unstable and so cannot be the ground state wherever Eq. (32) is violated for some α, $\mathbf{k}$.[16] Thus, the configuration is the ground state if and only if Eq. (32) is valid.

The above condition can conveniently be expressed in terms of matrices $\mathbf{K}(\mathbf{k})$ defined by

$$\mathbf{K}(\mathbf{k})=\mathfrak{D}'(\mathbf{k})-\lambda_{\min}(0)\mathbf{I}, \tag{33}$$

where $\mathbf{I}$ is the 6×6 unit matrix. The validity of Eq. (32) is equivalent to all the $\mathbf{K}(\mathbf{k})$ being positive semidefinite (having no negative eigenvalues), and the ground-state region $\mathfrak{R}$ consists of all parameter values for which no $\mathbf{K}(\mathbf{k})$ has a negative eigenvalue. Since any eigenvalue branch is a continuous function of $\mathbf{k}$, $\mathfrak{R}$ is bounded by surfaces where eigenvalues of particular $\mathbf{K}(\mathbf{k})$ matrices first become zero. Since the determinant of a matrix is equal to the product of its eigenvalues, these boundary surfaces can be determined by locating the zeros of the corresponding determinants $|\mathbf{K}(\mathbf{k})|$.

The examination of the entire Brillouin zone at every point in parameter being impractical, we shall first consider those k vectors parallel to the symmetry directions [001], [100], [110], and [101], together with the special k vector at the edge of the Brillouin zone in the [201] direction. For these particular cases, the functions $\chi(\mathbf{k})$, $\eta_i(\mathbf{k})$, and $\zeta_{ij}(\mathbf{k})$ assume the forms given in Appendix B, so that the matrices $\mathfrak{D}'(\mathbf{k})$ and $\mathbf{K}(\mathbf{k})$ can immediately be partially diagonalized by the choice of basis vectors indicated in Appendix B.[17] Because of this decomposition of the original 6×6 determinants into products of smaller ones, their zeros can be handled analytically to yield explicit equations for the corresponding boundary surfaces. The region enclosed by these surfaces will be called $\mathfrak{R}^{(0)}$ and must contain $\mathfrak{R}$ itself, i.e., $\mathfrak{R}$ can be no larger than $\mathfrak{R}^{(0)}$. Subsequent numerical investigation of $|\mathbf{K}(\mathbf{k})|$ over all $\mathbf{k}$ at points on the boundaries of $\mathfrak{R}^{(0)}$ then shows the fashion in which $\mathfrak{R}$ differs from $\mathfrak{R}^{(0)}$. It turns out that most of the boundary of $\mathfrak{R}$ coincides with that of $\mathfrak{R}^{(0)}$, with only small differences which occasionally occur in the corners of $\mathfrak{R}^{(0)}$.

From the information given in Appendix B, it is possible to write all the determinants of the various 2×2 and 3×3 submatrices for $\mathbf{k}$ in the specified symmetry directions in the form

$$\mathrm{Det}(k)=s^2(As^4+Bs^2+C), \tag{34}$$

where A, B, and C are explicit functions of t, u, v, and w where $s=\sin\sigma$ or $\sin\rho$, σ and ρ (from Appendix B) being proportional to k, the magnitude of $\mathbf{k}$. In general, the definition of a boundary surface requires that simultaneously $\mathrm{Det}(k)=0$ and $\partial\mathrm{Det}(k)/\partial k=0$. One possible solution yields the boundary equation $B^2-4AC=0$ corresponding to $s^2=-B/(2A)$. This solution can be valid only when $0\leq s^2\leq 1$. For $s^2=1$, the extrema condition is automatically satisfied, so that the boundary equation is simply $A+B+C=0$. Both of the above

[15] It is worth noting that the existence of simultaneous angles on A and B sites requires that either $\lambda_1=\lambda_2=\lambda_3=\lambda_5$ or $\lambda_1=\lambda_4=\lambda_5$. These degeneracies have been found to occur only along surfaces ($2tu=1$ and $4tuv=1$, respectively). Consequently, it is unlikely that such conditions will be met. We might note that no unique configuration is defined on these surfaces because they also yield degeneracy between physical configurations (e.g., S_{Y1} and S_{A1}) and arbitrary linear combinations of such degenerate configurations are possible.

[16] This theorem for coplanar configuration was proven in footnote 15 of reference 7.

[17] Although this partial diagonalization was accomplished here by inspection, general group theoretical methods can, of course, be employed. However, it appears that this diagonalization comprises the total extent to which group theory is useful in solving the classical ground-state problem.

conditions become identities for $s=0$, in which case the criterion $\partial^2 \mathrm{Det}(k)/\partial k^2=0$ yields the boundary equation $C=0$. The region $\mathfrak{R}^{(0)}$ is enclosed by the most stringent of the resulting boundary surfaces.

A. Néel Region ($\mathfrak{R}_N$)

In Sec. III A, we explicitly evaluated $\beta(t,u,v,w)=\beta_N$ and $\lambda_{\min}(0)=\lambda_N$ for the Néel configuration. These values define a particular set of matrices $\mathbf{K}(\mathbf{k})$ and thereby define the coefficients A, B, and C appearing in Eq. (34) as particular functions of t, u, v, and w. Then the procedure outlined above gives rise to a large number of equations for possible boundary surfaces corresponding to the various wave vector modes. Those which are pertinent to the determination of $\mathfrak{R}_N{}^{(0)}$ are given in Appendix C for $\mathbf{k}$ parallel to the [001], [100], [110], and [101] directions. These surfaces supplement the three already obtained in Sec. III A from consideration of the $\mathbf{k}=0$ modes alone, namely $2t=1$, $u=1$, and $2uv=1$. In addition, the boundary equation resulting from the special case where $\mathbf{k}=(1/2)$ [201] is included in Appendix C.

The higher order equations given in Appendix C have been solved numerically by means of an IBM 7090 computer. The complexity of the resulting region $\mathfrak{R}_N{}^{(0)}$ for $t=0$ (no A-A interaction) is illustrated in Fig. 3, which depicts that part of $\mathfrak{R}_N{}^{(0)}$ having $u\geq 0$, $-1\leq v\leq 1$, and $w\geq 0$. It can be seen that $\mathfrak{R}_N{}^{(0)}$ is bounded by a number of intersecting surfaces which arise from k vectors along the indicated symmetry directions and that it contains the parameter range ($u\leqslant 8/9$) along the "cubic line" ($v=1/2$, $w=1/3$) over which the Néel configuration is already known to be the ground state.[6] (The existence of the surface labeled [$0\epsilon\delta$] in Fig. 3 is inferred from the results obtained later in this section for $\mathfrak{R}_{Y2}$.) The effect of the A-A interaction is indicated by Fig. 4, where the intersections of $\mathfrak{R}_N{}^{(0)}$ with the planes $v=0$, $v=0.5$, and $v=1.0$ are shown for several values of t. Here the curves labeled $t=0$ correspond to the surfaces outlined in Fig. 3, and it is clear that small values of t (<0.1) produce little change in these surfaces. Since

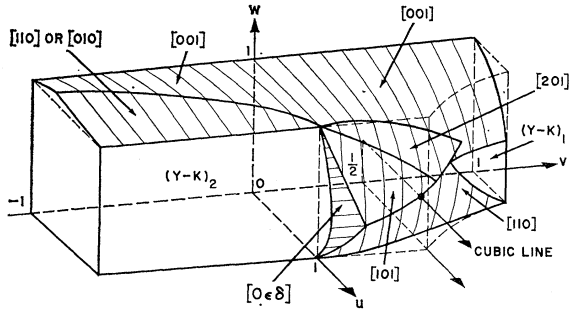

FIG. 3. The region $\mathfrak{R}_N{}^{(0)}$ for the Néel configuration for $t=0$, $u\geq 0$, $-1\leq v\leq 1$, and $w\geq 0$. The boundary surfaces arise from $\mathbf{k}$ vectors along the indicated directions.

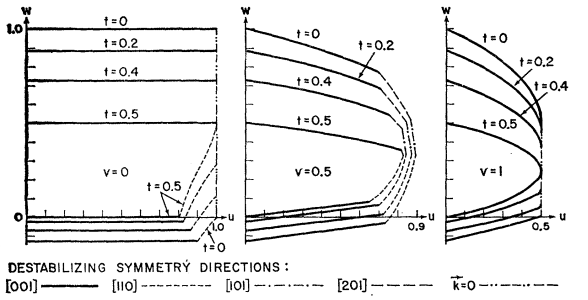

FIG. 4. The intersections of the Néel region $\mathfrak{R}_N{}^{(0)}$ with the planes $v=0$, 1/2, 1. The various curves give the boundaries for the indicated values of t.

A-A interactions appear experimentally to be small,[18] the surfaces shown in Fig. 3 should generally yield a good approximation for actual materials.[19]

In order to determine the true ground-state region $\mathfrak{R}_N$ contained within $\mathfrak{R}_N{}^{(0)}$, our procedure is to investigate $\mathbf{K}(\mathbf{k})$ over all $\mathbf{k}$ in the first Brillouin zone first along the boundary of $\mathfrak{R}_N{}^{(0)}$, and then at interior points where necessary. In this fashion, we find boundaries of $\mathfrak{R}_N$ for all $t\leq 0.5$ to be given by the [001] and $(Y\text{-}K)_1$ surfaces along their intersection, by the [110] and $(Y\text{-}K)_1$ surfaces along their intersection, and by the [010] and $(Y\text{-}K)_2$ surfaces along their intersections. Furthermore, for $t=0$ we find the [001] surface to be a valid boundary of $\mathfrak{R}_N$ when $u=0$ and $w=1$ for all v, and when $v=0$ and $w=1$ for all $u\leq 1$. We also find the $(Y\text{-}K)_2$ surface to be a valid boundary when $t=0$, $u=1$, and $v=0$ for $0\leq w\leq 1$. However, numerical calculations using an IBM 7090 computer show that $\mathfrak{R}_N$ deviates from $\mathfrak{R}_N{}^{(0)}$ when $v=1/2$, as indicated in Fig. 5, which should be compared with the corresponding cross section of $\mathfrak{R}_N{}^{(0)}$ given in Fig. 4. Taken all together, the above results suggest that the boundaries of $\mathfrak{R}_N$ probably coincide with those of $\mathfrak{R}_N{}^{(0)}$ except in the neighborhoods of the [201], [101], and (possibly) the [$0\epsilon\delta$] surfaces.

The boundaries shown in Fig. 5 which arise from k vectors in nonsymmetry directions have greater significance than indicated by the resulting slight reduction of $\mathfrak{R}_N$ from $\mathfrak{R}_N{}^{(0)}$, since they imply that, for (u,w) near such a boundary and outside of $\mathfrak{R}_N$, the ground-state spin configuration will contain a large Fourier component corresponding to $\mathbf{k}$ in such a nonsymmetry direction. (Judging from our cubic spinel results, this configuration might very well be a magnetic spiral.)

[18] J. M. Hastings failed to find any evidence of magnetic ordering in the neutron diffraction patterns from $CoAl_2O_4$ at temperatures down to 4.2°K (private communication). Since the classical ground state for antiferromagnetic nearest-neighbor A-A interactions is nondegenerate (there is no competition such as occurs for B-B interactions), Hasting's result indicates that $t<0.1$ for any cobalt spinel with $T_C\geq 40$°K. Estimates of large A-A interaction previously given in the literature are unreliable, since they were based upon the application of the Yafet-Kittel model to spinels for which it is invalid.

[19] Small values of t could lead to qualitative changes in the destabilizing $\mathbf{k}$ only if surfaces for different $\mathbf{k}$'s were nearly degenerate for $t=0$. Except near the intersections, such degeneracies do not occur in $\mathfrak{R}_N{}^{(0)}$.

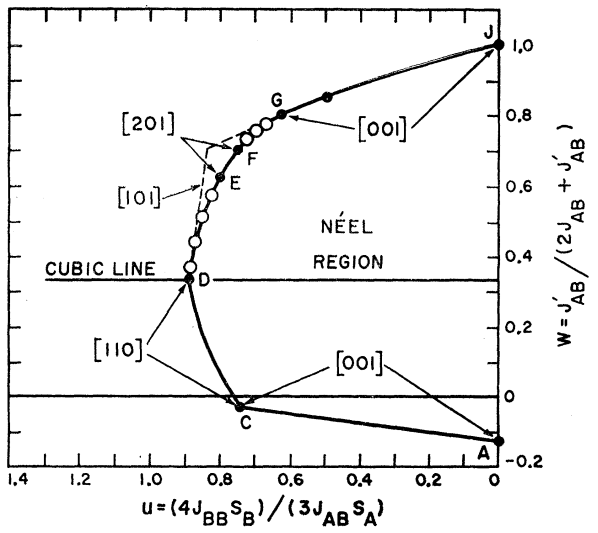

FIG. 5. The intersection of Néel ground-state region $\mathcal{R}_N$ with the plane $v=1/2$ for $t=0$. The destabilizing $\mathbf{k}$ vector is in the [001] direction from A to C, in the [110] from C to D, varies in direction from D to E, is in the [201] from E to F, varies from F to G, and remains in the [001] from G to J.

Consequently it is of interest to examine the variation of $\mathbf{k}$ in detail. Along the section of the boundary labeled J-G in Fig. 5, $\mathbf{k}$ points in the [001] direction and changes in length as indicated in Fig. 6, which depicts one octant of the first Brillouin zone. At the point G, a spiral configuration with $\mathbf{k}=(1/2)$ [111] becomes degenerate, so that infinitesimally past G towards F the destabilizing wave vector changes discontinuously, as shown in Fig. 6. On passing from G to F, $\mathbf{k}$ remains on the surface of the Brillouin zone, but varies continuously in direction from the [111] to the [201]. The section from F to E is simply part of the [201] boundary surface defined by Eq. (C 10). Then from E to D the wave vector varies continuously, remaining within the zone and attaining the [101] direction at the cubic line, where it becomes degenerate with another $\mathbf{k}$ of equal length pointing in the [110] direction. This latter $\mathbf{k}$ increases gradually in length as one progresses from D to C, at which point it reaches the edge of the Brillouin zone and becomes degenerate with a wave vector of zero length in the [001] direction. Along the remaining section from C to A, the Néel mode is destabilized by a long-wavelength spiral propagating in the [001] direction.

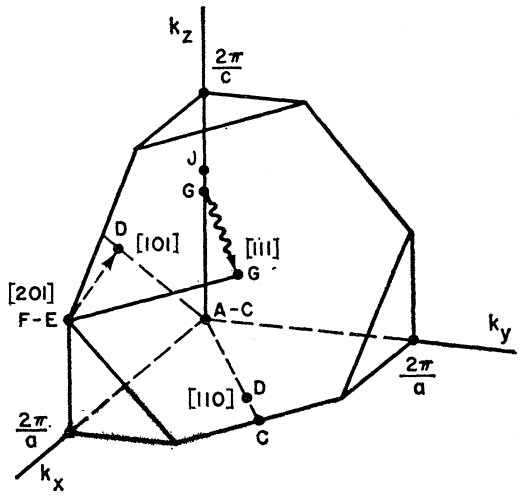

FIG. 6. One octant of the first Brillouin zone. The tip of the destabilizing k vector (see Fig. 5) follows the indicated path.

B. Yafet-Kittel Regions ($\mathcal{R}_{Yi}$)

The explicit functions $\beta(t,u,v,w)=\beta_{Yi}$ and $\lambda_{\min}(0)=\lambda_{Yi}$ given in Sec. III B yield the matrices $\mathbf{K}(\mathbf{k})$ appropriate to the Yafet-Kittel configurations. Calculation of the coefficients A, B, and C appearing in the boundary condition given by Eq. (34) then shows that the parameters t and u appear only as their product tu.

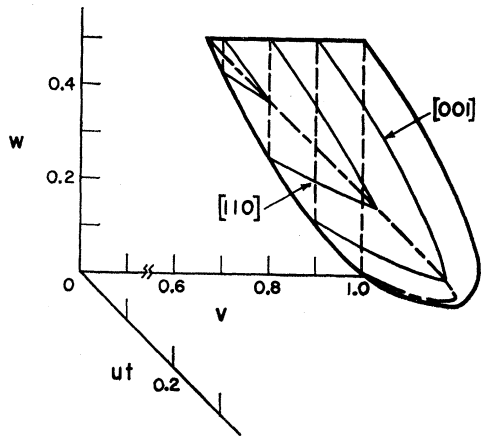

FIG. 7. The region $\mathcal{R}_{Y1}^{(0)}$ in the three-dimensional tu, v, w space. There is an additional restriction that $2uv\geq 1$.

This simplification permits the description of the ground-state regions $\mathcal{R}_{Yi}$ in terms of a three-dimensional parameter space defined by tu, v, and w.

1. Upon consideration of the boundary conditions for $\mathbf{k}$ in the same symmetry directions as before, we find $\mathcal{R}_{Y1}^{(0)}$ to be enclosed by the surfaces

$$tu=2w(1-2w)/v, \tag{35}$$

arising from the extrema $s^2=0$ for $\mathbf{k}=[00h]$, and

$$tu=2(w-1)(1-v-vw)/v(2v-1), \tag{36}$$

arising from the extrema $s^2=0$ for $\mathbf{k}=[hh0]$. All of the other possible boundary surfaces are less restrictive and, therefore, do not enter into the definition of $\mathcal{R}_{Y1}^{(0)}$. The surfaces given by Eqs. (35) and (36) are shown in Fig. 7 for $v\leq 1$, and some of the constant-v cross sections of the resulting $\mathcal{R}_{Y1}^{(0)}$ are illustrated in Fig. 8, where the wave-vector directions associated with the boundaries are indicated. However, it should be remembered from

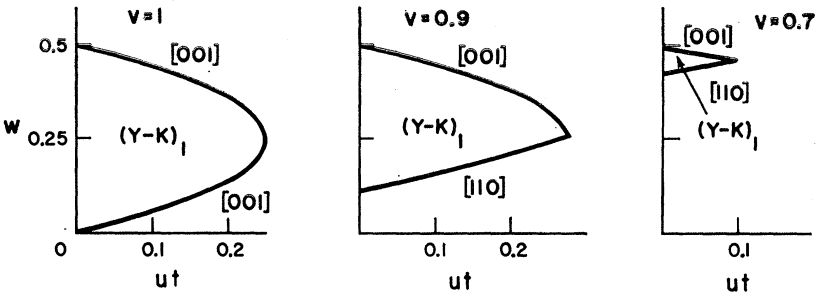

FIG. 8. Constant-v cross sections of $\mathcal{R}_{Y1}^{(0)}$, subject to restriction $2uv \geq 1$. Destabilizing $\mathbf{k}$-vector modes are indicated by brackets.

Eq. (21) that $\mathcal{R}_{Y1}$ can exist only when

$$2uv \geq 1, \tag{37}$$

and that appropriate matrices $\mathbf{K}(\mathbf{k})$ can be defined only when this condition is satisfied. Hence, Eq. (37) places an additional restriction upon the region $\mathcal{R}_{Y1}^{(0)}$.

The appropriate matrices $\mathbf{K}(\mathbf{k})$ were investigated over all $\mathbf{k}$ in the first Brillouin zone for $2/3 \leq v \leq 1$ using an IBM 7090 computer. Such a calculation for an interior point of $\mathcal{R}_{Y1}^{(0)}$ verified that all the eigenvalues were positive, and other calculations for several points on the boundary surfaces and at their intersections showed that $\mathcal{R}_{Y1} = \mathcal{R}_{Y1}^{(0)}$. These results prove rigorously that $\mathcal{S}_{Y1}$ is the classical ground state for all values of t, u, v, and w lying within the region $\mathcal{R}_{Y1}^{(0)}$ depicted in Figs. 7 and 8, subject to the additional constraint expressed by Eq. (37), and unstable outside of $\mathcal{R}_{Y1}^{(0)}$.

The above result has immediate application to the tetragonal spinel $CuCr_2O_4$, which is known to possess the $\mathcal{S}_{Y1}$ spin configuration.[10,11] In copper chromite, the c/a ratio is less than unity, so that one would expect to find $v > 1/2$, and values of v greater than $2/3$ (required by $\mathcal{R}_{Y1}$) would not appear unreasonable. However, a naive consideration of the A-B interaction for the actual degree of distortion leads one to expect w to be greater than $1/2$, which would be outside of $\mathcal{R}_{Y1}$. Hence, we conclude that, if copper chromite possesses only nearest-neighbor exchange interactions, then less obvious super-exchange mechanisms (e.g., π-bonding effects) must be present in the total A-B interaction.

2. According to the discussion in Sec. III B, the $\mathcal{S}_{Y2}$ configuration can only exist when $v < 1/2$. For this case, consideration of $\mathbf{k}$ in the various symmetry directions leads to a single boundary surface for $\mathcal{R}_{Y2}^{(0)}$,

$$tu = 2w(1-w), \tag{38}$$

which is independent of v. This surface arises from the $s^2 = 1$ extremum for $\mathbf{k} = [h00]$, although it is "accidentally" degenerate with a $[hh0]$ boundary when $v = 0$ and with a $[00h]$ boundary when both $v = 0$ and $w \geq 1/2$. The resulting region $\mathcal{R}_{Y2}^{(0)}$ is illustrated in Fig. 9 for $-1 \leq v \leq 0$, but is subject to the additional restriction that

$$u \geq 1 \tag{39}$$

in order for $\mathcal{S}_{Y2}$ to exist [from Eq. (24)].

Numerical investigation of $\mathbf{K}(\mathbf{k})$ over the first Brillouin zone at an interior point of $\mathcal{R}_{Y2}^{(0)}$ showed all the eigenvalues to be positive, and calculations at a number of points along the surface defined by Eq. (38) showed that $\mathcal{R}_{Y2} = \mathcal{R}_{Y2}^{(0)}$ for $-1 \leq v \leq 0$. Other calculations for small positive values of v showed that $\mathcal{R}_{Y2}$ is first destabilized by a $\mathbf{k} = [0\epsilon\delta]$, where both ϵ and δ approach zero on the boundary. As shown in Appendix D, this situation can be treated analytically to yield the boundary

$$2v = [2w(1-w) - tu]/[2(1+3w) - tu]. \tag{40}$$

This complicated surface has the properties that $v = 0$ along the $[h00]$ boundary given by Eq. (38) and that everywhere $0 \leq v \leq v_{\max}$, where $v_{\max} = 0.055$ and occurs when both $tu = 0$ and $w = 1/3$. The direction of $\mathbf{k}$ is defined by the ratio δ/ϵ, which varies over the surface (from Appendix D) so that $\mathbf{k}$ is not confined to symmetry directions over this boundary. The configuration $\mathcal{S}_{Y2}$ will be the ground state within the region $\mathcal{R}_{Y2}$ defined by Eqs. (38) and (40), subject to the restriction of Eq. (39), and will be unstable outside this region.

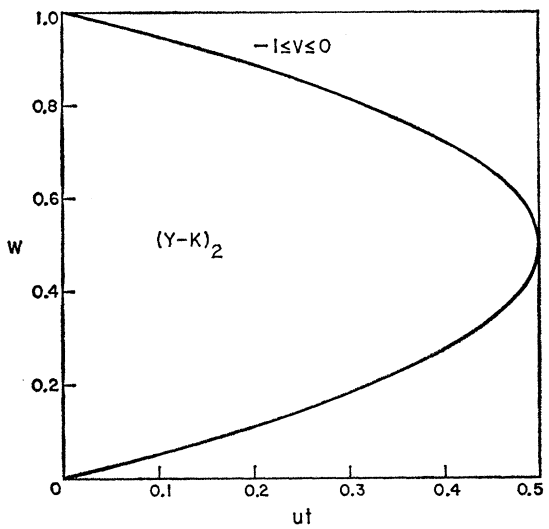

FIG. 9. The region $\mathcal{R}_{Y2}^{(0)}$ for $-1 \leq v \leq 0$. There is an additional restriction that $u \geq 1$. Destabilizing surface arises from $\mathbf{k} = [h00]$ mode.

Since hausmannite (Mn_3O_4) apparently possesses a spin configuration characterized by a $\mathbf{k}=[hh0]$,[20] and since it has a c/a ratio greater than unity so that presumably $v<1/2$, it had been hoped that a part of the $\mathcal{R}_{Y2}$ boundary would arise from such a wave vector. As can be seen from Fig. 9, this is not the case. Although $\mathcal{R}_{Y2}$ is destabilized by a spiral with $\mathbf{k}=[h00]$ rather than by one with $\mathbf{k}=[hh0]$, the exchange energy difference between the two latter types of configurations is very small for small negative values of v. Therefore, one cannot exclude the possibility that the large anisotropy forces known to exist in hausmannite[21] may lower the total magnetic energy of the [110] configuration below that of the [100] along part of the boundary.

3. In Sec. III B, we found that the configuration $\mathcal{S}_{Y3}$ could exist only for $t\geq 1/2$. Since it appears that actual spinels probably possess values of t less than 0.1, we shall not consider this case further.

C. Antiferromagnetic Regions ($\mathcal{R}_{Ai}$)

The appropriate expressions for β_{Ai} and λ_{Ai} for the two possible antiferromagnetic configurations were obtained in Sec. III C. The configuration $\mathcal{S}_{A1}$ is possible only when $v\geq 1/2$, and consideration of its corresponding $\mathbf{K}(\mathbf{k})$ for $\mathbf{k}=[00h]$ immediately restricts its region $\mathcal{R}_{A1}{}^{(0)}$ to the surface $w=1/4$. Since the ground-state region R_{A1} must be included in $\mathcal{R}_{A1}{}^{(0)}$, it cannot enclose any volume in our (four-dimensional) parameter space, and will not be considered further. In other words, we find that $\mathcal{S}_{A1}$ occurs only as a special case of an antiferromagnetic [001] spiral whose wavelength becomes infinite for $w=1/4$.

Similarly, $\mathcal{R}_{A2}$ is possible only for $v\leq 1/2$, and consideration of its $\mathbf{K}(\mathbf{k})$ for $\mathbf{k}=[h00]$ immediately restricts $\mathcal{R}_{A2}{}^{(0)}$ to the surface $w=1/2$. Consequently $\mathcal{R}_{A2}$ is also of zero volume, and the configuration $\mathcal{S}_{A2}$ occurs only as a special case of an antiferromagnetic [100] spiral whose wavelength becomes infinite for $w=1/2$. The detailed treatment of these spiral configurations will be left to a later paper.

V. HIGH-TEMPERATURE EFFECTS ($T=T_c$)

In the preceding sections, we have obtained those regions of parameter space within which the $\mathbf{k}=0$ modes are the classical ground state ($T=0$), and outside of which they are unstable. It is also of interest to examine the corresponding stability regions for temperature in the neighborhood of the highest transition temperature T_c. For temperatures slightly less than T_c, use of the molecular field approximation leads[22] to the eigenvalue equation

$$\langle\mathbf{Q}_\nu(\mathbf{k})\rangle=[-2(2\bar{J}_{AB}+\bar{J}_{AB}')/(3kT)]\times\sum_\mu \mathbf{L}_{\nu\mu}'(\mathbf{k})\langle\mathbf{Q}_\mu(\mathbf{k})\rangle, \quad (41)$$

where the $\langle\mathbf{Q}_\nu(\mathbf{k})\rangle$ are the Fourier transforms of the average spin vectors $\langle\mathbf{S}_{n\nu}\rangle$ according to Eq. (6) and where the matrices $\mathbf{L}'(\mathbf{k})$ are given by Eq. (10). Nonzero solutions of Eq. (41) exist only when $-3kT/[2(2\bar{J}_{AB}+\bar{J}_{AB}')]$ is equal to an eigenvalue of $\mathbf{L}'(\mathbf{k})$, so that T_c (the highest temperature for which a nonzero solution exists) is uniquely associated with the minimum eigenvalue of $\mathbf{L}'(\mathbf{k})$. Then the corresponding eigenvector defines the spin configuration appropriate to T_c. Note that the strong constraints, and hence the adjustable parameters β, do not enter into the high-temperature problem, i.e., the $\langle\mathbf{S}_{n\nu}\rangle$ are not required to be unit vectors.

An investigation of the high-temperature properties of the $\mathbf{k}=0$ modes must start from the eigenvalues and eigenvectors of $\mathbf{L}'(0)$, which can be obtained from Table I and Eqs. (14), (15), and (16) by setting $\beta=1$. Since the adjustable parameter β is no longer available to force degeneracies, the only ferrimagnetic configuration possible at T_c arises from Ψ_1 and is of the Néel type. At T_c, the other eigenvectors involved in the construction of the three $\mathcal{S}_{Yi}$ configurations at $T=0$ give rise instead to three antiferromagnetic configurations $\mathcal{S}_{dAi}$, in which the spins are ordered on only one type of site (A or B) and disordered on the other, as described by Lotgering.[14] Comparison of the associated eigenvalues ($\lambda_N=\lambda_1$, $\lambda_{dA1}=\lambda_4$, $\lambda_{dA2}=\lambda_2=\lambda_3$, and $\lambda_{dA3}=\lambda_5$) shows that λ_N lies lowest inside a region bounded by the surfaces

$$0=u^2v(3v-1)+4tuv-2, \quad (42)$$

$$0=u^2(1-v)+4tu-4, \quad (43)$$

$$0=4t^2+tu(1+v)-1. \quad (44)$$

These boundary surfaces arise from $\mathcal{S}_{dAi}$ with $i=1$, 2, and 3, respectively, and the first two are compared with the corresponding ground-state boundaries for $t=0$ and $0\leq v\leq 1$ in Fig. 10. The significant feature of this comparison is the increased stability at T_c of the Néel configuration relative to the other $\mathbf{k}=0$ modes for this portion of parameter space.

All the high-temperature boundary equations are more complicated than their ground-state analogues, since the appropriate expressions for λ do not work out as simply. For this reason, we have only examined the symmetry directions [001], [100], and [110]. The resulting outer limits $\mathcal{R}^{(0)}(T_c)$ to the true stability regions $\mathcal{R}(T_c)$ are qualitatively similar to those obtained in Sec. IV for the ground-state problem, the same general portions of their boundaries arising from the same symmetry directions. For example, both $\mathcal{R}_{dA1}{}^{(0)}(T_c)$ and $\mathcal{R}_{Y1}{}^{(0)}(0)$ are bounded only by surfaces with $\mathbf{k}=[00h]$ for $t=0$ and $v>1$ plus an additional surface associated with $\mathbf{k}=[hh0]$ for smaller v, and both $\mathcal{R}_N{}^{(0)}(T_c)$ and $\mathcal{R}_N{}^{(0)}(0)$ possess a boundary arising from $\mathbf{k}=[hh0]$ in the neighborhood of $t=0$, $v=1/2$, and $w=1/3$, as shown in Fig. 10. The principle differences between $\mathcal{R}(T_c)$ and

[20] J. S. Kasper, Bull. Am. Phys. Soc. 4, 178 (1959).
[21] K. Dwight and N. Menyuk, Phys. Rev. **119**, 1470 (1960).
[22] See Appendix VI of reference 7.

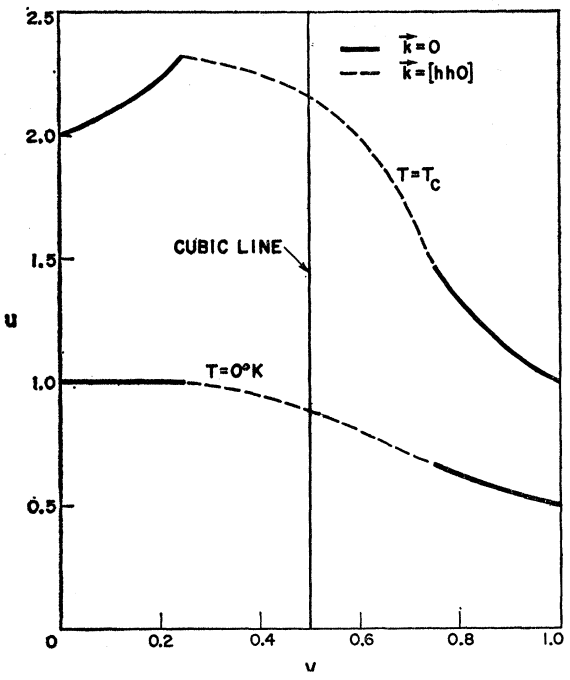

FIG. 10. Comparison between high-temperature and ground-state stability boundaries of the Néel configuration for $t=0$, $w=1/3$, and $0\leq v\leq 1$. The destabilizing modes are as indicated.

$\mathfrak{R}(0)$ for $t=0$ are that the w extents of $\mathfrak{R}_{dA1}(T_c)$ and $\mathfrak{R}_{dA2}(T_c)$ increase with increasing u instead of remaining constant, and that $\mathfrak{R}_N(T_c)$ has a greater extent in u (though not in w) than $\mathfrak{R}_N(0)$.

Since the high-temperature spin configuration of a tetragonal spinel must arise from a single eigenvector of $\mathbf{L}'(\mathbf{k})$, an antiferromagnetic configuration must either be an antiferromagnetic spiral if $\mathbf{k}\neq 0$ or one of the $\mathfrak{R}_{dAi}$ if $\mathbf{k}=0$, whereas a ferrimagnetic configuration must be of the Néel type with $\mathbf{k}=0$. Thus Lotgering's findings[14] can be generalized to state that in tetragonal spinels neither Yafet-Kittel nor ferrimagnetic-spiral configurations can exist at the highest transition temperature. Consequently, ferrimagnetic material with noncollinear ground states must possess at least two transitions, as has been discussed in detail elsewhere for the case of manganese chromite.[7]

VI. SUMMARY AND CONCLUSIONS

In this paper, we have considered normal spinels which possess nearest-neighbor *A-A*, *A-B*, and *B-B* exchange interactions that conform to tetragonal symmetry and which, therefore, can be characterized by points in a four-dimensional parameter space. By application of the generalized Luttinger-Tisza method, we have determined those regions of this parameter space within which the various $\mathbf{k}=0$ modes are the classical ground state. Only a spinel characterized by a point inside one of these regions can, on the basis of exchange alone, evidence the corresponding spin configuration at absolute zero.

These regions are much smaller than predicted by previous[1,3,14] theories which are restricted entirely to $\mathbf{k}=0$ spin configurations (although in the present paper only $\mathbf{k}=0$ configurations were investigated as possible ground states, their stability relative to *all* configurations has been included in our theory). Consequently, experimental knowledge of the existence of one of these states gives correspondingly more information as to values of the exchange parameters. The example of copper chromite was discussed in this connection.

The $\mathbf{k}=0$ modes become unstable along the boundary surfaces of their ground-state regions because of spin deviations associated with some particular propagation vectors $\mathbf{k}$ which characterize the surfaces. The determination of these destabilizing k vectors has been included as a significant part of this investigation. In particular, it is found that the Néel configuration, for certain values of the exchange parameters, is destabilized by $\mathbf{k}$'s which are not parallel to symmetry directions. Therefore, it is almost certain that ground-state spin configurations exist in which there is an important Fourier component corresponding to $\mathbf{k}$ in nonsymmetry directions. Furthermore, the application of similar considerations to the case of hausmannite (Mn_3O_4) indicates that anisotropy forces must be invoked in order to account for the observed spin configuration in this material.

In addition to our treatment of the ground-state ($T=0$) problem, we have investigated the stabilities of the $\mathbf{k}=0$ modes at high temperatures ($T=T_c$) by means of the molecular field approximation. It was found that the onset of ferrimagnetism immediately below the highest magnetic transition temperature can only correspond to a Néel-type configuration. All the other possible configurations, whether collinear or spiral, are antiferromagnetic. It follows that the existence of a Yafet-Kittel or ferrimagnetic-spiral ground-state configuration requires the existence of at least two magnetic transitions. This situation appears to exist in manganese chromite.[8]

ACKNOWLEDGMENTS

We are pleased to acknowledge the help of Mrs. Ann Sherman and Mrs. Margaret G. Durgin in all aspects of our work involving the use of the IBM 7090 computer, and to express our appreciation for the encouragement of J. B. Goodenough throughout the entire course of this research. We would also like to thank J. Hastings for permitting us to discuss the results of his neutron diffraction experiments on cobalt aluminate prior to publication.

APPENDIX A. THE MATRIX ELEMENTS

Throughout this paper, vectors will be referred to the pseudocubic tetragonal unit cell, the cell edges being denoted by a and c. Furthermore, we shall

denote vectors in the direct space by $\mathbf{R}_{nv}=(rst)$ where we define $(rst)=(a/8)[r\hat{x}+s\hat{y}+t(c/a)\hat{z}]$, and vectors in reciprocal space by $\mathbf{k}=[hkl]$ with the definition $[hkl]=(2\pi/a)[h\hat{x}+k\hat{y}+l(a/c)\hat{z}]$. In this notation, $\mathbf{k}\cdot\mathbf{R}_{nv}=(\pi/4)(hr+ks+lt)$.

The evaluation of the functions χ, η_i, and ζ_{ij} follow straightforwardly from the definitions given by Eqs. (4), (9), and (10), together with Fig. 1. For example, $t\chi=L_{12}'(\mathbf{k})$ and

$$(2\bar{J}_{AB}+\bar{J}_{AB}')L_{12}'(\mathbf{k})=\bar{J}_{AA}\{\exp[i\mathbf{k}\cdot(222)]+\exp[i\mathbf{k}\cdot(2\bar{2}\bar{2})]+\exp[i\mathbf{k}\cdot(\bar{2}2\bar{2})]+\exp[i\mathbf{k}\cdot(\bar{2}\bar{2}2)]\}.$$

Since $\bar{J}_{AA}=t(2\bar{J}_{AB}+\bar{J}_{AB}')$, one obtains

$$\chi=\exp[i\mathbf{k}\cdot(222)]+\exp[i\mathbf{k}\cdot(2\bar{2}\bar{2})]+\exp[i\mathbf{k}\cdot(\bar{2}2\bar{2})]+\exp[i\mathbf{k}\cdot(\bar{2}\bar{2}2)]. \quad \text{(A1)}$$

The functions η_1 arise from the A-B interactions. For example, $\eta_1=L_{13}'(\mathbf{k})$ and

$$(2\bar{J}_{AB}+\bar{J}_{AB}')L_{13}'(\mathbf{k})=\bar{J}_{AB}\{\exp[i\mathbf{k}\cdot(31\bar{1})]+\exp[i\mathbf{k}\cdot(\bar{1}3\bar{1})]\}+\bar{J}_{AB}'\exp[i\mathbf{k}\cdot(\bar{1}13)].$$

From Eq. (4) it follows that $\bar{J}_{AB}=\frac{1}{2}(1-w)(2\bar{J}_{AB}+\bar{J}_{AB}')$ and $\bar{J}_{AB}'=w(2\bar{J}_{AB}+\bar{J}_{AB}')$. Thus,

$$\eta_1=\tfrac{1}{2}(1-w)\{\exp[i\mathbf{k}\cdot(31\bar{1})]+\exp[i\mathbf{k}\cdot(\bar{1}3\bar{1})]\}+w\exp[i\mathbf{k}\cdot(\bar{1}13)]. \quad \text{(A2)}$$

Similar considerations yield

$$\eta_2=\tfrac{1}{2}(1-w)\{\exp[i\mathbf{k}\cdot(\bar{3}\bar{1}\bar{1})]+\exp[i\mathbf{k}\cdot(13\bar{1})]\}+w\exp[i\mathbf{k}\cdot(1\bar{1}3)], \quad \text{(A3)}$$

$$\eta_3=\tfrac{1}{2}(1-w)\{\exp[i\mathbf{k}\cdot(\bar{3}11)]+\exp[i\mathbf{k}\cdot(1\bar{3}1)]\}+w\exp[i\mathbf{k}\cdot(11\bar{3})], \quad \text{(A4)}$$

$$\eta_4=\tfrac{1}{2}(1-w)\{\exp[i\mathbf{k}\cdot(3\bar{1}1)]+\exp[i\mathbf{k}\cdot(\bar{1}31)]\}+w\exp[i\mathbf{k}\cdot(\bar{1}\bar{1}3)]. \quad \text{(A5)}$$

For the B-B interactions, we note that $2\bar{J}_{BB}=u(1-v)\times(2\bar{J}_{AB}+\bar{J}_{AB}')$ and $2\bar{J}_{BB}'=uv(2\bar{J}_{AB}+\bar{J}_{AB}')$. Since, for example,

$$(2\bar{J}_{AB}+\bar{J}_{AB}')L_{34}'(\mathbf{k})=\bar{J}_{BB}\{\exp[i\mathbf{k}\cdot(2\bar{2}0)]+\exp[i\mathbf{k}\cdot(\bar{2}20)]\}=2\bar{J}_{BB}\cos[\mathbf{k}\cdot(2\bar{2}0)]$$

and $u(1-v)\zeta_{12}=L_{34}'(\mathbf{k})$, one obtains

$$\zeta_{12}=\cos[\mathbf{k}\cdot(2\bar{2}0)]. \quad \text{(A6)}$$

Similarly it can be shown that

$$\zeta_{13}=\cos[\mathbf{k}\cdot(202)], \quad \text{(A7)}$$

$$\zeta_{14}=\cos[\mathbf{k}\cdot(02\bar{2})], \quad \text{(A8)}$$

$$\zeta_{23}=\cos[\mathbf{k}\cdot(022)], \quad \text{(A9)}$$

$$\zeta_{24}=\cos[\mathbf{k}\cdot(20\bar{2})], \quad \text{(A10)}$$

$$\zeta_{34}=\cos[\mathbf{k}\cdot(220)]. \quad \text{(A11)}$$

APPENDIX B. REDUCTION OF $K(k)$ FOR k IN SYMMETRY DIRECTIONS

1. For $\mathbf{k}=[00h]$, it is convenient to define $\sigma=\pi h/4$. Then the expressions given in Appendix A become

$$\chi=4\cos(2\sigma), \quad \text{(B1)}$$

$$\eta_1=\eta_2=\eta_3^*=\eta_4^*=(1-w)\exp(-i\sigma)+w\exp(+3i\sigma), \quad \text{(B2)}$$

$$\zeta_{12}=\zeta_{34}=1, \quad \text{(B3)}$$

$$\zeta_{13}=\zeta_{14}=\zeta_{23}=\zeta_{24}=\cos(2\sigma). \quad \text{(B4)}$$

The corresponding matrices $\mathfrak{L}'(\mathbf{k})$ and $\mathbf{K}(\mathbf{k})$ can be partially diagonalized into 1×1 and 2×2 submatrices with the following basis vectors: $(1\times1)_1$ with

$$\psi_1=(1/\sqrt{2})(0,0,1,-1,0,0);$$

$(1\times1)_2$ with

$$\psi_2=(1/\sqrt{2})(0,0,0,0,1,-1);$$

$(2\times2)_1$ between

$$\psi_3=(1/\sqrt{2})(1,1,0,0,0,0)$$

and

$$\psi_4=(1/2)(0,0,1,1,1,1);$$

and $(2\times2)_2$ between

$$\psi_5=(1/\sqrt{2})(1,-1,0,0,0,0)$$

and

$$\psi_6=(1/2)(0,0,1,1,-1,-1).$$

2. For $\mathbf{k}=[h00]$, with σ defined as above, one obtains similarly

$$\chi=4\cos(2\sigma), \quad \text{(B5)}$$

$$\eta_1=\eta_2^*=\eta_3^*=\eta_4=\tfrac{1}{2}(1-w)\times[\exp(-i\sigma)+\exp(+3i\sigma)]+w\exp(-i\sigma), \quad \text{(B6)}$$

$$\zeta_{14}=\zeta_{23}=1, \quad \text{(B7)}$$

$$\zeta_{12}=\zeta_{13}=\zeta_{24}=\zeta_{34}=\cos(2\sigma). \quad \text{(B8)}$$

Again the 6×6 matrices decompose into 1×1 and 2×2 submatrices, namely, $(1\times1)_1$ with

$$\psi_1=(1/2)(0,0,1,1,-1,-1);$$

$(1\times1)_2$ with

$$\psi_2=(1/2)(0,0,1,-1,1,-1);$$

$(2\times2)_1$ between

$$\psi_3=(1/\sqrt{2})(1,1,0,0,0,0)$$

and

$$\psi_4=(1/2)(0,0,1,1,1,1);$$

and $(2\times2)_2$ between

$$\psi_5=(1/\sqrt{2})(1,-1,0,0,0,0)$$

and

$$\psi_6=(1/2)(0,0,1,-1,-1,1).$$

3. For $\mathbf{k}=[hh0]$, we define $\rho=\pi h/2$. Then

$$\chi=2(1+\cos 2\rho)=4\cos^2\rho, \tag{B9}$$

$$\eta_1=\eta_2=w+(1-w)\cos(2\rho), \tag{B10}$$

$$\eta_3=\eta_4{}^*=\cos\rho-i(1-2w)\sin\rho, \tag{B11}$$

$$\zeta_{12}=1, \tag{B12}$$

$$\zeta_{34}=\cos(2\rho). \tag{B13}$$

$$\zeta_{13}=\zeta_{14}=\zeta_{23}=\zeta_{24}=\cos\rho. \tag{B14}$$

In this case partial diagonalization yields a 1×1, a 2×2, and a 3×3 submatrix: the (1×1) for

$$\psi_1=(1/\sqrt{2})(0,0,1,-1,0,0);$$

the (2×2) connecting

$$\psi_2=(1/\sqrt{2})(1,-1,0,0,0,0)$$

and

$$\psi_3=(1/\sqrt{2})(0,0,0,0,1,-1);$$

and the (3×3) for

$$\psi_4=(1/\sqrt{2})(1,1,0,0,0,0),$$

$$\psi_5=(1/\sqrt{2})(0,0,1,1,0,0),$$

and

$$\psi_6=(1/\sqrt{2})(0,0,0,0,1,1).$$

4. For $\mathbf{k}=[h0h]$, with ρ defined as above, one obtains:

$$\chi=4\cos^2\rho, \tag{B15}$$

$$\eta_1=\eta_3{}^*=\cos\rho+iw\sin\rho, \tag{B16}$$

$$\eta_2=\eta_4{}^*=\tfrac{1}{2}(1-w)+\tfrac{1}{2}(1+w)\cos(2\rho)-\tfrac{1}{2}i(1-3w)\sin(2\rho), \tag{B17}$$

$$\zeta_{12}=\zeta_{14}=\zeta_{23}=\zeta_{34}=\cos\rho, \tag{B18}$$

$$\zeta_{13}=\cos(2\rho), \tag{B19}$$

$$\zeta_{24}=1. \tag{B20}$$

The original 6×6 matrices can then be decomposed into two 3×3 submatrices: $(3\times3)_1$ connecting

$$\psi_1=(1/\sqrt{2})(1,1,0,0,0,0),$$

$$\psi_2=(1/\sqrt{2})(0,0,1,0,1,0),$$

and

$$\psi_3=(1/\sqrt{2})(0,0,0,1,0,1);$$

and $(3\times3)_2$ connecting

$$\psi_4=(1/\sqrt{2})(1,-1,0,0,0,0),$$

$$\psi_5=(1/\sqrt{2})(0,0,1,0,-1,0),$$

and

$$\psi_6=(1/\sqrt{2})(0,0,0,1,0,-1).$$

5. At the edge of the Brillouin zone in the [201] direction, $\mathbf{k}=(1/2)[201]$. Writing $\tau=\pi/8$, it follows that

$$\chi=2[\cos(2\tau)+\cos(6\tau)], \tag{B21}$$

$$\eta_1=\eta_3{}^*=\tfrac{1}{2}(1-w)[\exp(5i\tau)+\exp(-3i\tau)]+w\exp(i\tau), \tag{B22}$$

$$\eta_2=\eta_4{}^*=\tfrac{1}{2}(1-w)[\exp(i\tau)+\exp(-7i\tau)]+w\exp(5i\tau), \tag{B23}$$

$$\zeta_{12}=\zeta_{34}=\cos(4\tau), \tag{B24}$$

$$\zeta_{13}=\cos(6\tau), \tag{B25}$$

$$\zeta_{14}=\zeta_{23}=\zeta_{24}=\cos(2\tau). \tag{B26}$$

The resulting partial diagonalization is identical with that given above for case 4.

APPENDIX C. BOUNDARIES OF $\mathfrak{R}_N{}^{(0)}$

The boundary equations $2t-1=0$, $u-1=0$, and $2uv-1=0$ were obtained in Sec. III A from the consideration of the $\mathbf{k}=0$ modes alone. For $\mathbf{k}=[00h]$, the procedure described in Sec. IV yields the additional boundary equations

$$2uv-(1+8w-2t)=0, \tag{C1}$$

$$t^2u^2v^2+4w[2w(1-t)-t]uv+8w^2[2w(w-1)+t]=0, \tag{C2}$$

corresponding to $s^2=0$ and $s^2=(4w^2+2w-tuv)/(8w^2)$, respectively, where it is to be remembered that Eq. (C2) is valid only when $0\leq s^2\leq1$. For $\mathbf{k}=[h00]$, the additional surfaces are given by

$$u-(5-2t-4w)=0, \tag{C3}$$

$$t^2u^2-4(1-w)[t-(1-w)(1-t)]u+4(1-w)^2\times[(1-w)^2-2(1-w)+2t]=0, \tag{C4}$$

corresponding to $s^2=0$ and $s^2=[2(1-w)(2-w)-tu]/[4(1-w)^2]$, respectively. For both of the above symmetry directions, the extrema $s^2=1$ yields no new information.

For $\mathbf{k}=[hh0]$, consideration of the extremum $s^2=1$ leads to the boundary

$$2v(1-t)u^2+[2t(1+v)-(1+2v)-4w(1-w)]u+[1-2t+4w(1-w)]=0, \tag{C5}$$

whereas consideration of the general condition gives

$$\begin{aligned}t^2v^2u^4&-\{2tv[t(1-v)+2v(3-4w+w^2)-2(1-w)]\\&+8v(1-v)(1-w)^2\}u^3\\&-\{4(1-v)(1-w)^2(4tv+8vw-10v-1)-4tv(1-w^2)\\&-[t(1-v)+2v(3-4w+w^2)-2(1-w)]^2\}u^2\\&-4(1-w)^2\{t(1-v)+2v(2-4w+w^2)\\&-(1-v)(2t+4w-5)-2(1-w)\}u\\&+4(1-w)^4=0,\end{aligned} \tag{C6}$$

corresponding to

$$s^2=\{tvu^2-u[t(1-v)-2(1-2v)(1-w)+2v(1-w)^2]+2(1-w)^2\}/[4u(1-v)(1-w)^2].$$

In this case the surface obtained from the extremum $s^2=0$ has already been given by Eq. (C3).

For $\mathbf{k}=[h0h]$, the extrema $s^2=0$ and $s^2=1$ yield, respectively,

$$u(1+2v)-[4(1+w)+2(1-2t)]=0, \quad \text{(C7)}$$

$$(2-u)(1-t)-w^2=0. \quad \text{(C8)}$$

The general solution, valid only for $0\leq s^2\leq 1$ as in Eqs. (C2), (C4), and (C6) above is

$$\begin{aligned} &t^2(1+2v)^2u^4-2(1+2v)\{t[3+4w-4vw+w^2-4v(1-t)] \\ &\quad +4v(1+w)^2\}u^3+\{[3+4w-4vw+w^2-4v(1-t)]^2 \\ &\quad +4(1+w)^2[t(1-6v)+2v(7+4w+2v)]\}u^2 \\ &\quad -4(1+w)^2\{3+4w+4vw+w^2+8v-4vt\}u \\ &\qquad +4(1+w)^4=0, \end{aligned} \quad \text{(C9)}$$

corresponding to

$$\begin{aligned} s^2=\{&tu^2(1+2v)-u[(4tv+2(1-2v)(1+w)+(1+w)^2] \\ &+2(1+w)^3\}/[4uv(1+w)^2]. \end{aligned}$$

Finally, consideration of the particular wave vector $\mathbf{k}=(1/2)[201]$ gives

$$\begin{aligned} &(1-t)(1+2v)u^2-[4(1-t)(1-v)-w^2]u \\ &\qquad +[4(1-t)-2w^2]=0. \end{aligned} \quad \text{(C10)}$$

The surfaces defined by all the above equations enclose a region in t, u, v, w parameter space, this region being called $\mathcal{R}_N{}^{(0)}$.

APPENDIX D. ANALYTIC CALCULATION FOR $k=[0\varepsilon\delta]$

For this case, evaluation of the expressions for χ, η_i, and ζ_{ij} given in Appendix A yields

$$\chi=4(1-2\sin^2\bar{\epsilon})(1-2\sin^2\bar{\delta}), \quad \text{(D1)}$$

$$\begin{aligned} \eta_1=\eta_3{}^*=w\exp[i(\bar{\epsilon}+3\bar{\delta})]+\tfrac{1}{2}(1-w) \\ \times\{\exp[i(\bar{\epsilon}-\bar{\delta})]+\exp[-i(3\bar{\epsilon}+\bar{\delta})]\}, \end{aligned} \quad \text{(D2)}$$

$$\begin{aligned} \eta_2=\eta_4{}^*=w\exp[i(-\bar{\epsilon}+3\bar{\delta})]+\tfrac{1}{2}(1-w) \\ \times\{\exp[-i(\bar{\epsilon}+\bar{\delta})]+\exp[i(3\bar{\epsilon}-\bar{\delta})]\}, \end{aligned} \quad \text{(D3)}$$

$$\zeta_{12}=\zeta_{34}=\cos(2\bar{\epsilon}), \quad \text{(D4)}$$

$$\zeta_{14}=\zeta_{23}=\cos(2\bar{\delta}), \quad \text{(D5)}$$

$$\zeta_{13}=\cos 2(\bar{\epsilon}-\bar{\delta}), \quad \text{(D6)}$$

$$\zeta_{24}=\cos 2(\bar{\epsilon}+\bar{\delta}), \quad \text{(D7)}$$

where $\bar{\epsilon}=\pi\epsilon/4$ and $\bar{\delta}=\pi\delta/4$. The resulting 6×6 matrix can then be partially diagonalized into two 3×3 submatrices, this decomposition being identical with that given for case 4 in Appendix B. It turns out that $(3\times 3)_1$ is the submatrix of interest.

Since the numerical calculations indicated that the boundary arises when $\mathbf{k}\to 0$, we shall take $\bar{\epsilon}$ and $\bar{\delta}$ to be small, and expand the above functions as Taylor series in $\bar{\epsilon}$ and $\bar{\delta}$. Subsequent evaluation of $|\mathbf{K}(\mathbf{k})|$ for the submatrix $(3\times 3)_1$ leads to a power series in $\bar{\epsilon}^2$, $\bar{\delta}^2$, and $\bar{\epsilon}\bar{\delta}$, with

$$|\mathbf{K}(\mathbf{k})|^{(0)}=|\mathbf{K}(\mathbf{k})|^{(2)}=0, \quad \text{(D8)}$$

where the superscript refers to the total order in $\bar{\epsilon}$ and $\bar{\delta}$. The first nonzero term occurs in fourth order, and is given by

$$\begin{aligned} |\mathbf{K}(\mathbf{k})|^{(4)}/(8\beta^2u)=&\bar{\epsilon}^4(1-2v)[8(1-w)-4tu] \\ &+\bar{\epsilon}^2\bar{\delta}^2[8w(1-w)-4tu-2v(8+24w-4tu)]. \end{aligned} \quad \text{(D9)}$$

The coefficient of $\bar{\epsilon}^4$ will always be positive within the region $\mathcal{R}_{Y2}{}^{(0)}$ defined by Eq. (38), but the coefficient of $\bar{\epsilon}^2\bar{\delta}^2$ can become negative, in which case a negative value can be obtained for $|\mathbf{K}(\mathbf{k})|$ for a large enough ratio of δ to ϵ. Thus, a stability boundary arises when this latter coefficient equals zero, as given by Eq. (40). As one crosses through this boundary, the ratio δ/ϵ which minimizes $|\mathbf{K}(\mathbf{k})|$ changes, meaning that the direction of $\mathbf{k}$ changes.